Anal. Bioanal. Electrochem., Vol. 12, No. 1, 2020, 1-20

Analytical &
Bioanalytical
Electrochemistry

2020 by CEE
www.abechem.com

Full Paper

New Vitreous Phase as Mild Steel Inhibitors in Hydrochloric Acid

Ghizlane Ghenimi, Moussa Ouakki,* Hanane Barebita, Asmae El Fazazi, Taoufik Guedira and Mohammed Cherkaoui

Laboratory of materials, Electrochemistry and environment, Faculty of Science, Ibn Tofail University, PB. 133-14050 Kenitra, Morocco

*Corresponding Author, Tel.: +212611749011

E-Mail: moussassaw@gmail.com

Received: 17 October 2019 / Received in revised form: 21 December 2019 /
Accepted: 23 December 2019 / Published online: 31 January 2020

Abstract- Corrosion inhibition of mild steel by two new glassy materials correlated with the ternary system Bi_2O_3-B_2O_3-P_2O_5 in HCl 1.0 M medium was evaluated using different technics: Gravimetry and electrochemical methods (polarization and electrochemical impedance spectroscopy (EIS)). The results show that the inhibition efficiency depends on the concentration of the two compounds studied (1BHP, 2BHP) and the temperature. The adsorption model obeys to Langmuir isotherm. Thermodynamic parameters were calculated and analysed. The morphology of the steel surface was characterized by scanning electron microscopy (SEM) coupled with EDX.

Keywords- Glassy phase, Inhibition, Corrosion, Mild steel

1. INTRODUCTION

Steels are widely used in many fields because of their beneficial properties: good ductility, high tensile strength, good electrical and thermal conductivity and great ease of implementation [1,2]. However, steels are sensitive to corrosion. Their durability has been the subject of many researches these last year’s [3]. The use of inhibitors is one of the most effective methods in order to protect them from corrosion.

In industry, chloride acid solutions are usually used to eliminate the scale and stripping materials [4]. Acid must be treated to prevent a significant metal dissolution. This treatment involves the addition of certain organic or inorganic inhibitors such as Triazole, phosphates, polyphosphates, particularly metaphosphate glass, silicates and borates. These compounds will adsorb on the surface by the intermediate of heteroatoms: Azote (N), Oxygen (O), Sulfur (S) and sometimes phosphor (P) [5].

In literature, many phosphates derivatives and glassy phase compounds were studied as corrosion inhibitors and showed their effectiveness [6-8]. G. Saha et al. have studied the adsorption of the complex iron phosphates and figured out that only the surface of the iron hydroxides is combined with phosphate ions; no trace of calcium was detected in the complex iron phosphates [9,10].

The eco-friendly inhibition property of phosphate' compounds, in agreement with new environmental restrictions, makes them favorable for a practical use, as a replacement of certain toxic organic inhibitors [11,12]. As well as the use of glassy phases for the corrosion protection of steel [6].

The present study aims to evaluate the inhibition properties of two compounds based on phosphorous pentoxide P_2O_5, bismuth oxide Bi_2O_3 and boric acid H_3BO_3, namely 1BHP and 2BHP, on the corrosion of mild steel in HCl 1.0 M. The made up compounds were characterized by infrared spectroscopy. The effect of temperature on the electrochemical parameters of the system was studied as well, in order to define the adsorption mechanism of the studied compounds.

2. MATERIALS AND METHODS

2.1. Preparation of samples

Glassy phosphates were prepared from bismuth oxide Bi_2O_3, boric acid H_3BO_3 and diammonium hydrogen phosphate $(NH_4)_2HPO_4$ by stoichiometric mixture of raw materials according to the following reaction (1) [13]:

$$(1\text{-}x\text{-}y)\ Bi_2O_3\text{-}y\ H_3BO_3\text{-}\ x\ 2[(NH_4)_2HPO_4] \rightarrow (1\text{-}x\text{-}y)\ Bi_2O_3\ +y\,\frac{1}{2}\,B_2O_3 + xP_2O_5 \qquad (1)$$

The weighed materials were mixed and crushed in an Agat mortar. The thermic operation is realized in porcelain crucibles. The first treatment at 350 °C for 15 h enables hydrogen decomposition, it is followed by a grinding for homogenization. Each reaction mixture is then melted in an oven at 1050 °C, energetically plunged into a preheated aluminum mould at 200 °C [6]; and then stored in desiccators to avoid moisture. The compositions studied are collected in Table 1:

Table 1. Composition of glassy elements studied within the system

$(1\text{-x-y})\ Bi_2O_3 + y\frac{1}{2}\ B_2O_3 + xP_2O_5$			
Echa. N°	(1-x-y)	y	x
1BHP	0.55	0.35	0.10
2BHP	0.45	0.45	0.10

The aggressive solutions of HCl 1.0 M were prepared from HCl with an analytical quality (37% in weight). The concentrations of the two studied compounds were fixed from 50 to 300 ppm. The studied samples are of mild steel, with the chemical composition shown in Table 2. They were cut into 2.00 cm*1.00 cm* 0.20 cm plates for gravimetric tests. For electrochemical experiences, the mild steel samples were used with an exposed area of 1.0 cm² to the acid solution. Before each use, the samples were abraded with emery paper with different grades (from 180 to 1500), rinsed with distilled water, degreased with ethanol and air-dried.

Table 2. Chemical composition of mild steel (wt %)

Element	C	Si	Mn	S	P	Fe
wt (%)	0.17	0.20	0.37	0.03	0.01	Balance

2.2. Gravimetric tests

The samples were immerged for 6 h in HCl 1.0 M at 298 K in the absence and presence of the two compounds 1BHP and 2BHP then dried [14]. The loss weight is used to calculate the corrosion rate expressed in ($mg.cm^{-2}.h^{-1}$), using the following equation (2) [15]:

$$CR = \frac{W}{St} \tag{2}$$

W is the loss weight of the mild steel sample, S the surface exposed to the study solution and t the immersion time (6h).
The inhibition efficiency, $\eta_{CR}\%$, is determined as follow (3) [16]:

$$\eta\ CR\% = \frac{CR-CR\ (inh)}{CR} * 100 \tag{3}$$

where CR and $CR_{(inh)}$ represent the corrosion rate in the absence and presence of inhibitors, respectively.

2.3. Electrochemical cell

The electrochemical measurements were realized in a conventional three-electrode cell with a working electrode of steel plate with an exposed surface of 1 cm^2, a Pt counter electrode and an Ag/AgCl/KCl saturated reference electrode.

The working electrode was immerged in the prepared solutions for a half an hour until a stable open circuit potential is achieved (Eocp). All the electrochemical experiments were realized at a temperature of 298 K. The potential area is from -900 to -100 mV/Ag/AgCl with a scan rate of 1 mV/s.

In order to evaluate the kinetic parameters of corrosion, an adjustment with the Stern-Geary equation was used [17]. For the potential area not too far from the open circuit potential, we can consider that both processes followed Tafel's law [17], which is derived from (4):

$$i= i_a + i_c = i_{corr} \{\exp[b_a*(E - E_{corr})] - \exp[b_c*(E - E_{corr})]\} \quad (4)$$

where $\mathbf{i_{corr}}$ is the corrosion current density ($A.cm^{-2}$), b_a and b_c are the anodic and the cathodic Tafel constants, respectively (V^{-1}). Those constants are linked to Tafel slopes β (V/dec) at the usual logarithmic scale given by the equation (5):

$$\beta = \frac{ln10}{b} = \frac{2.303}{b} \quad (5)$$

The kinetic parameters of corrosion were then evaluated using the non-linear least squares method with Origin software. The potential range applied was limited to ±100 mV/Ag/AgCl around the E_{corr}, in order to avoid a significant systematic divergence sometimes observed for anodic and cathodic branches.

The corrosion inhibition efficiency was evaluated from the corrosion current density values, according to (6):

$$\eta_{pp\%}= [(i^0_{corr} - i_{corr})/ i^0_{corr}]*100 \quad (6)$$

where i^0_{corr} and i_{corr} are the corrosion current density values in the absence and presence of inhibitors, respectively

The SEM measurements were done with amplitude of ±10 mV, in a frequency range from 100 KHz to 100 mHz with ten points per decade.

The results were then analyzed and an equivalent electric circuit was determined using Bouckamp program [18]. The inhibition efficiency, derived from EIS, $\eta_{EIS}\%$ was also added and calculated using the following equation (7):

$$\eta_{EIS}\% = [(R_{ct} - R^0_{ct}) / R_{ct}]*100 \quad (7)$$

Where R_{0ct} and R_{ct} are the values of charge transfer resistance in the absence and presence of both compounds 1BHP and 2BHP.

2.4. Surface analysis

Steel surface characterization before and after 6 h of immersion in HCl 1,0 M solution, in the absence and presence of both compounds studied 1BHP and 2BHP at 298 K, was realized owing to the Scanning Electron Microscopy (SEM). The elemental analysis is obtained by coupling the system with an energy dispersive analysis (EDX). These analyses were realized in the research center CAC of Cadi-Ayyad University in Marrakech.

3. RESULTS AND DISCUSSION

3.1. Gravimetric measurements

Corrosion rate (CR) and inhibition efficiency (η_{CR}%) values, obtained from the weight loss measurements, are shown in Table 3. Observation of the table revealed that the corrosion rate decreases, while the inhibition efficiency increases with the decrease in inhibitors' concentrations. η_{CR}% reached a maximum value of 79.8% and 86.2%, with a concentration of 50 ppm, for both compounds 1HBP and 2HBP, respectively.

Table 3. Corrosion rate and inhibition efficiency in 1.0 M HCl 1.0 M solution

Medium	**Concentration (ppm)**	**CR (mg/cm^2 .h)**	**η_{CR} (%)**
HCl 1.0 M	**--**	7.65	-
1BHP	**50**	1.62	78.8
	100	1.68	78.0
	200	1.76	76.9
	300	2.09	72.7
2BHP	**50**	1.05	86.2
	100	1.23	83.9
	200	2.14	72.1
	300	2.55	66.7

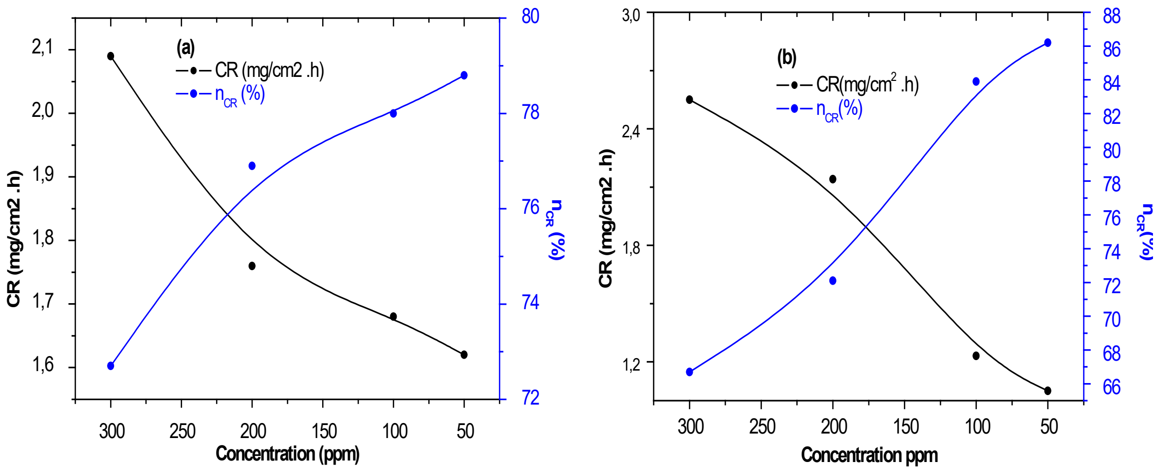

Fig. 1. Corrosion rate and inhibition efficiency variation for mild steel as a function of the concentration of the two glassy compounds 1BHP (a) and 2BHP (b) in HCl 1.0 M medium

3.2. Electrochemical study

3.2.1. Potentiostatic study

Polarization plots for mild steel in 1.0 M HCl with and without different concentrations of 1BHP and 2BHP at 298 °K are shown in Figure 2. Electrochemical parameters such as the corrosion potential E_{corr}(mV/Ag/AgCl), the cathodic and anodic slopes βc and βa, the corrosion current density i_{corr} and the inhibition efficiency η_{PP}% are reported in Table 4.

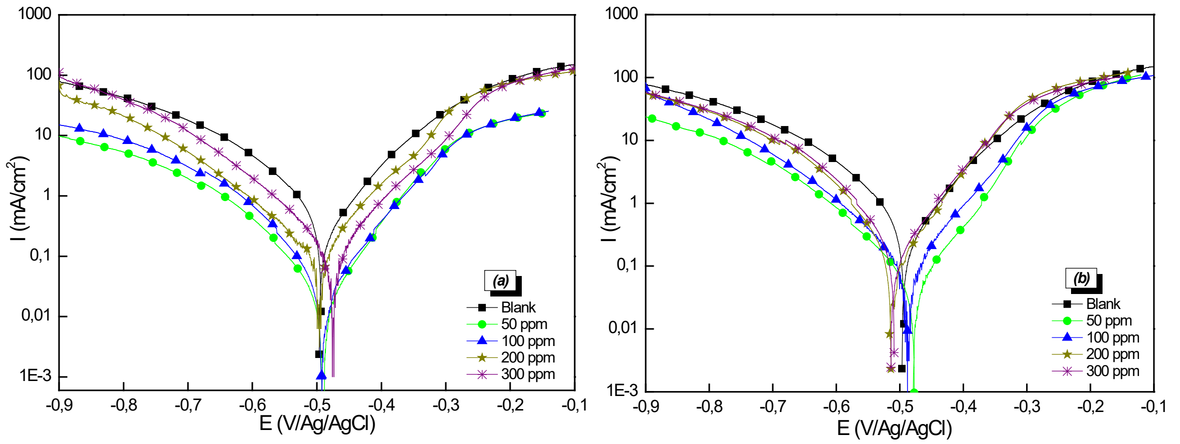

Fig. 2. Polarization plots for mild steel in 1.0 M HCl in the absence and presence of the glassy compounds 1BHP (a) and 2BHP (b) at 298 K

Figure 2 shows that the addition of the two glassy compounds induces a decrease in the cathodic and anodic current densities. The cathodic plots present a large domain of linearity indicating that Tafel law is verified. The discharge of H^+ proton is then takes place according to a pure activation kinetic.

The values of the cathodic and anodic Tafel slopes (Table 4) suggest that the reactional mechanism of hydrogen reduction remains unchanged in the absence and presence of 1BHP and 2BHP. Involving a significant decrease in the corrosion current, to achieve a value, thus inhibitory efficacy is equal to 78.9% and 86.6% to 50 ppm for both 1BHP and 2BHP compounds respectively.

Table 4. Electrochemical parameters and inhibition efficiency of steel corrosion in HCl 1.0 M without and with the addition of different concentrations of the glassy compounds at 298 K

Medium	**Conc. ppm**	**$-E_{corr}$ mV/Ag/AgCl**	**i_{corr} µA cm^{-2}**	**$-\beta_c$ mV dec^{-1}**	**β_a mV dec^{-1}**	**Θ**	**η_{PP} %**
HCl 1.0 M	--	498	983	140	150	-	-
1BHP	50	489	207	131	124	0.789	78.9
	100	490	220	136	132	0.776	77.6
	200	497	231	123	130	0.765	76.5
	300	469	267	120	129	0.728	72.8
2BHP	50	472	132	121	128	0.866	86.6
	100	484	155	132	142	0.842	84.2
	200	511	275	136	135	0.720	72.0
	300	507	332	128	136	0.662	66.2

The addition of the compounds in the electrolyte has also caused the variation of E_{corr} values, the displacement is superior to 85 mV, and thus, the inhibitor could be considered as a cathodic or anodic type [19-21]. If the variation is lower than 85 mV, the inhibitor can be considered as a mixed type inhibitor [22]. The maximum displacement in this study was of +30 mV, indicating that both compounds are mixed type inhibitors.

This result could indicate that the inhibitory action occurred simply by blocking the cathodic and anodic sites available on the surface of the metal. By adsorption of inhibitor molecules on the surface of the steel [23,24].

3.2.2. EIS studies

The corrosion behavior of mild steel in HCl 1.0 M solution in the absence and presence of different concentrations of 1BHP and 2BHP was studied using EIS, after 30 min of immersion in HCl 1.0 M corrosive solution at 298 K. Nyquist plots with open circuit potential are shown in Figure 3. The plots are two imperfect semicircles for both inhibitors, indicating that the corrosion mechanism of mild steel is under charge transfer mechanism [25-27].

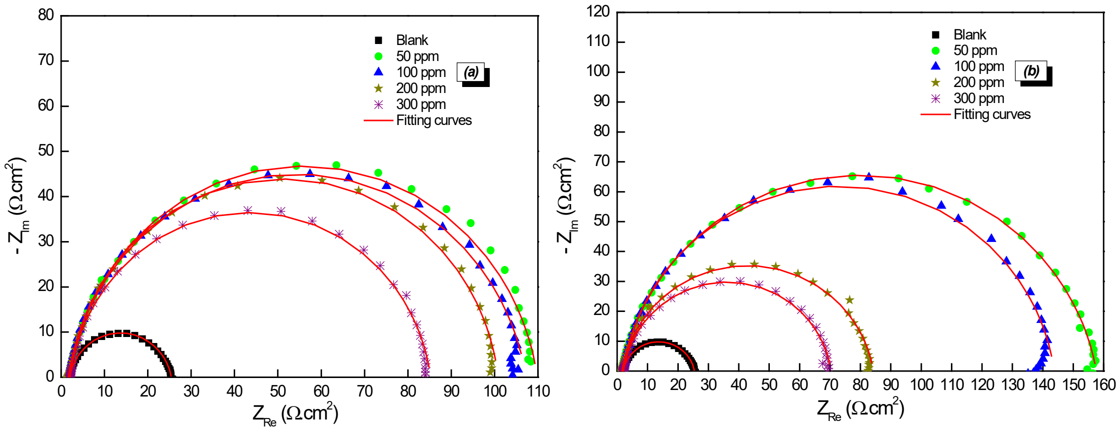

Fig. 3. Nyquist plots obtained for mild steel after 30 min of immersion in HCl 1.0 M solution with different concentrations of 1BHP (a) and 2BHP (b) compounds at 298 K

The equivalent electric circuit presented in Figure 4, was proposed to simulate the experimental data. This circuit enables the identification of the solution resistance (R_s) and the charge transfer resistance (R_{ct}). It should be noted that the value of the double layer capacity (C_{ct}) was affected by the surface imperfections, this effect was simulated via a constant phase element (CPE) [28,29] and their parameters were calculated according to different models and are listed in Table 5.

Fig. 4. Equivalent circuits compatible with experimental impedance data

The CPE impedance is defined by two values, Q and n and it is described by the equation (8) [30,31]:

$$Z_{CPE} = Q^{-1}(j\omega)^{n} \tag{8}$$

where Q is the CPE constant, ω is the angular frequency ($rad.s^{-1}$), j is an imaginary number defined by $j^2=-1$ and n is a CPE exponent which can be used as an heterogeneity indicator or the surface roughness [32,33].The double-layer capacity values were calculated using the following equation (9):

$$C_{dl} = Q(2\pi w_{max})^{\alpha-1} \tag{9}$$

where $w_{max} = 2\pi f_{max}$ and f_{max} is the maximum frequency.

Table 5. Impedance parameters for mild steel corrosion in HCl 1.0 M in the absence and the presence of different concentrations of two glassy phase compounds at 298 K

	Conc. (M)	**R_s (Ω cm^2)**	**R_{ct} (Ω cm^2)**	**C_{dl} (μF.cm^{-2})**	**n_{dl}**	**Q (μF.S^{n-1})**	**η_{imp} %**
HCl 1.0 M	--	1.9	23.36	190	0.897	470	-
1BHP	50	1.8	108.9	90	0.902	184	78.5
	100	1.8	103.6	110	0.911	164	77.4
	200	1.9	98.9	125	0.924	235	76.4
	300	2.0	83.2	96.4	0.916	144	71.9
2BHP	50	1.5	157	100	0.872	170	85.1
	100	1.8	143.6	119	0.904	176	83.7
	200	1.6	81.75	139	0.908	209	71.4
	300	2.1	68.24	145	0.913	803	65.7

The data presented in Table 5 indicates that R_{ct} value increases in the presence of different concentrations of both inhibitors. Moreover, the value of the proportional factor Q of CPE varies in the usual way with the concentration of1BHP and 2BHP. This is attributed to the increase in surface coverage of mild steel by the inhibitory molecules leading to increased inhibition efficiency [34]. The increase in R_{ct} value is attributed to the formation of a protective layer in the metal/solution interface. It should be noted that the inhibition efficiencies calculated from electrochemical measurements are reasonably in agreement with those obtained from weight loss measurements.

Bode plots of mild steel immerged in HCl 1.0 M medium without and with different concentrations of 1BHP and 2BHP at 298 K are presented in Figure 5.

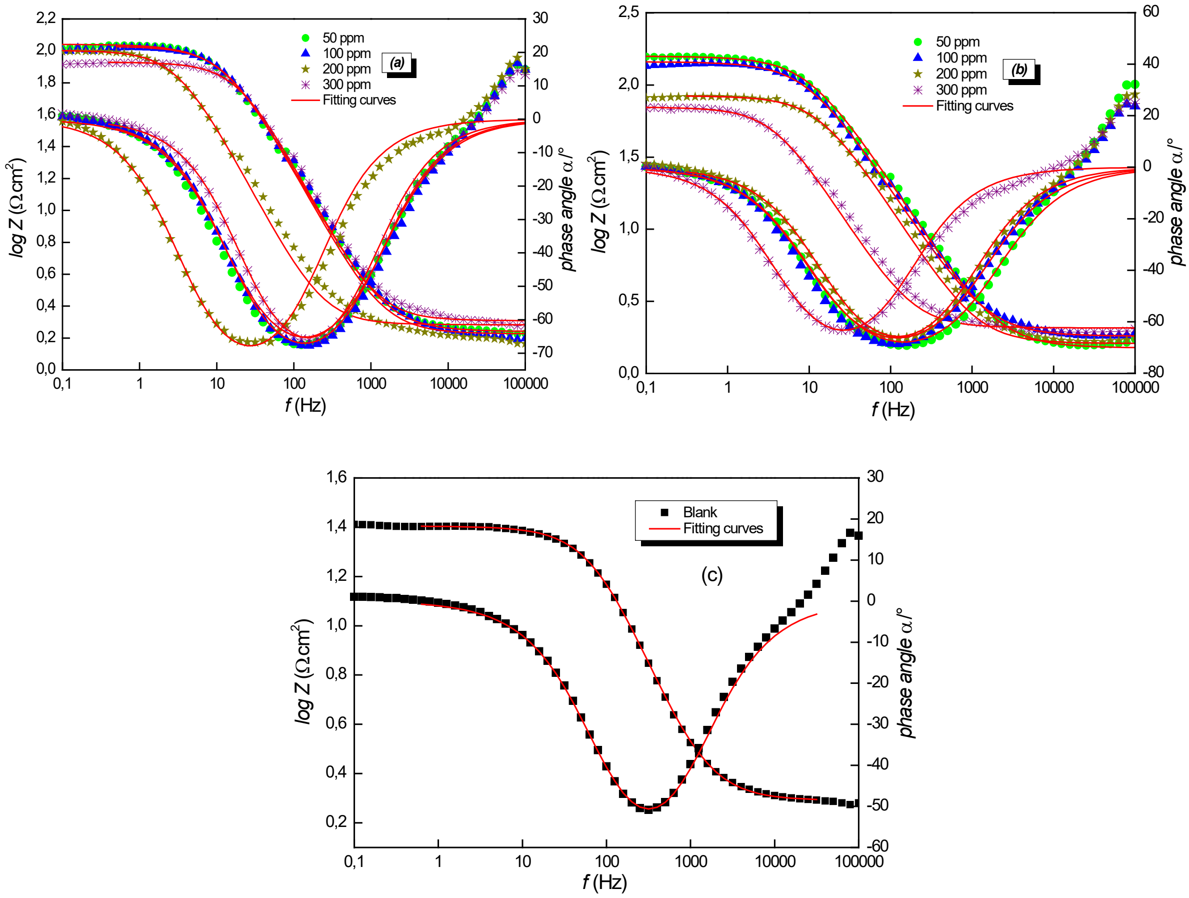

Fig. 5. Bode plots of mild steel immerged in HCl 1.0 M medium without (c) and with different concentrations of 1BHP (a) and 2BHP (b) at 298 K

In Bode plots, there is only one peak in both inhibitors as well as the blank solution, this result confirms the equivalent circuit model used to simulate the impedance spectrums. Bode plots show a single maximum phase for both inhibitors, indicating that the electrochemical process in the metal-solution interface is controlled by charge transfer kinetics.

3.2.3. Isothermal adsorption and temperature effect

The inhibition of metal corrosion by organic or inorganic compounds is due to their adsorption on the metal surface, which may involve two types of interaction with a metal surface (physisorption, chemisorption). The adsorption process therefore depends on the charge, the nature of the metal surface, the chemical structure of the inhibitor and the type of electrolyte [35]. However, several adsorption isotherms are generally used to describe the adsorption process, including Temkin, Frumkin, Langmuir and Flory-Huggins [36-39]. The best fit is obtained with the Langmuir isotherm. Adsorption of the inhibitor molecules to the surface of mild steel by the Langmuir adsorption isotherm is given by the accompanying conditions [40].

$$k_{ads}c_{inh} = \frac{\theta}{1-\theta} \tag{10}$$

where θ is the recovery rate, C_{inh} is the concentration of both glassy compounds and K_{ads} is the adsorption equilibrium constant. The linear curves of (C_{inh}/θ) as a function of the concentration of 1BHP and 2BHP are graphically presented according to the appropriate adsorption isotherm (Figure 6).

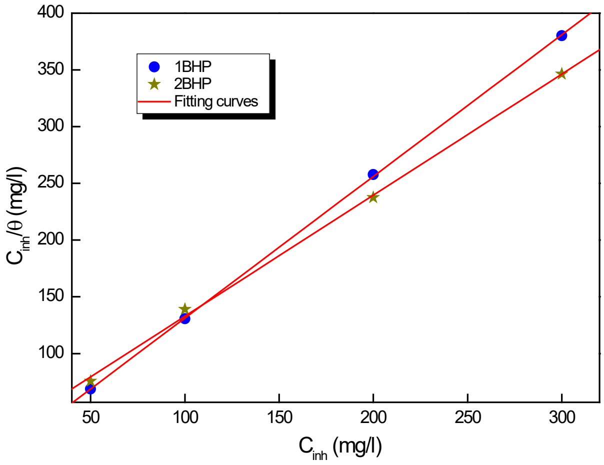

Fig. 6. The adsorption of Langmuir's isotherm of mild steel in HCl 1.0 M in the presence of the glassy compounds1BHP and 2BHP at 298 K

The coefficient of linear correlation (0.99997 for 1HBP and 0.99933 for 2HBP) are almost equal to 1 and the slopes of the lines are of 1.24881 for 1HBP and of 1.06746 for 2HBP, confirming the hypothesis that the adsorption of both glassy compounds obeys the adsorption of Langmuir's isotherm. It confirms the adsorption activity of two vitreous compounds on the mild steel surface, indicating that the typical adsorption sites at the steel-electrolyte interface are occupied by active compounds of 1BHP and 2BHP, as some works have reported [41]. So the adsorption equilibrium constant K_{ads}, is related to the free adsorption energy ΔG_{ads}, by the following equation (11) [42]:

$$K_{ads} = \frac{e^{(\frac{-\Delta G_{ads}}{RT})}}{C_{water}} \tag{11}$$

where, C_{water} is the concentration of the solution water (10^6 mg/L), R is the noble gases constant and T is the absolute temperature (K).

ΔG_{ads} values are calculated and grouped in Table 6. The negative values of the free adsorption energy ΔG_{ads}, indicate a spontaneous adsorption of both glassy compounds on the metallic surface as well as the strong interaction between the inhibitor molecules and the surface of mild steel [43,44].

In general, ΔG_{ads} values near to -20 KJ mol^{-1} or lower, are associated with electrostatic interaction between the charged molecules and the charged metal surface (physical adsorption);

while those near to –40 kJ mol^{-1} or higher, involve load sharing or transfer of inhibitor molecules to the surface of the metal to form a coordinated covalent bond (Chemical adsorption) [44-46]. ΔG_{ads} calculated values are between -20 kJ mol^{-1}and -40 kJ mol^{-1} for both products, suggesting that the adsorption of both inhibitors on the steel surface is of mixed type, predominantly physical (Table 6).

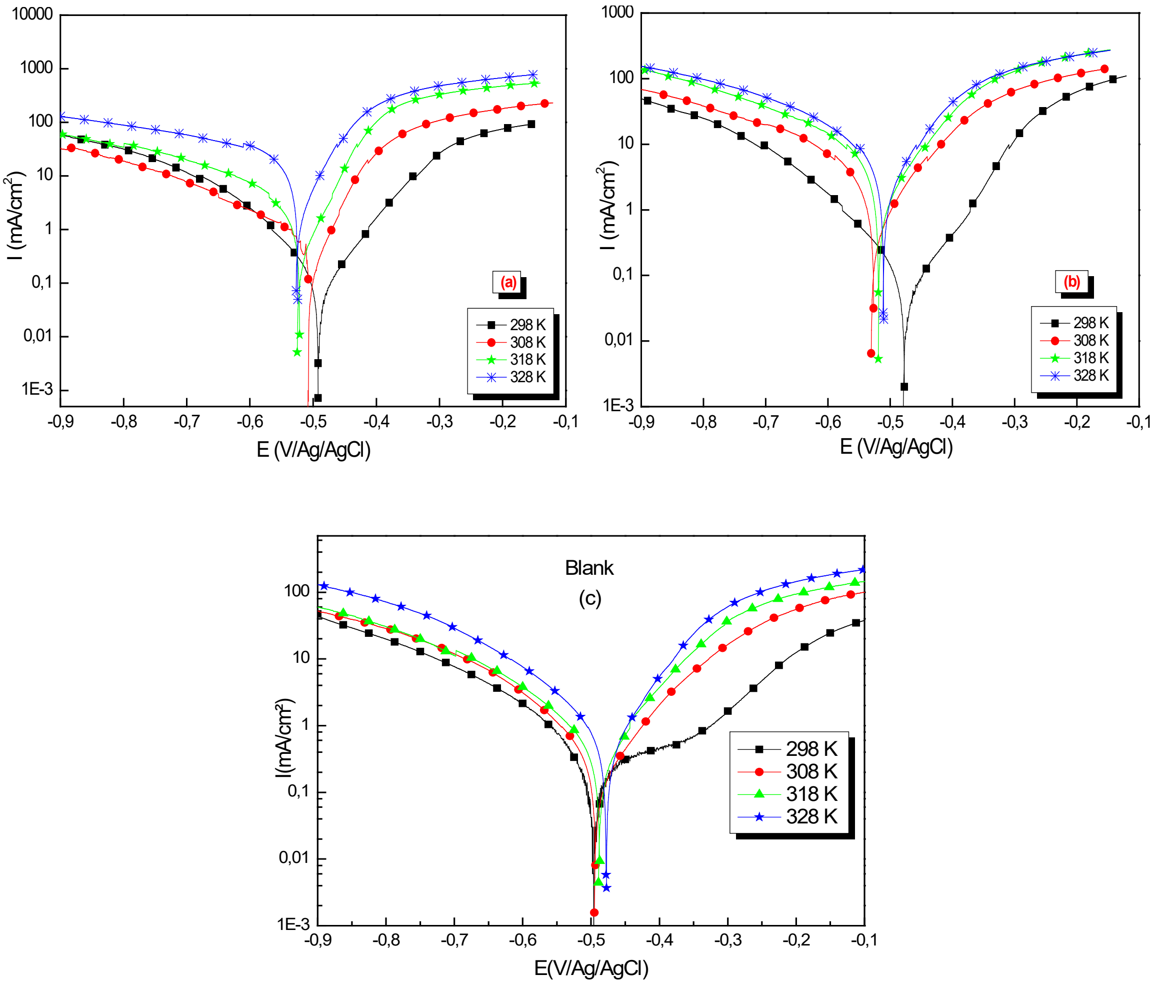

Fig. 7. Potentiostatic polarization plots of mild steel in HCl 1.0 M without (c) and with the addition of 50 ppm of 1HBP (a) and 2HBP (b) at different temperatures

Table 6. Thermodynamic parameters obtained from the adsorption of Langmuir's isotherm for both products at 298 K

Inhibitors	**K_{ads}(L /mol)**	**ΔG_{ads}(Kj/mol)**	**R^2**	**Slopes**
1 HBP	0.156	-29.6	0.99997	1.24881
2 HBP	0.038	-26.1	0.99933	1.06746

Generally, temperature is a factor that has a direct influence on the kinetics of chemical reactions in solution. According to literature, temperature may cause a change in the behavior of steel in a corrosive environment and in the nature of metal/inhibitor interaction [47]. In order to determine the effect of this variable on the inhibitory power of both glassy compounds (1BHP, 2BHP) on mild steel, we performed stationary electrochemical characterization in potentiostatic mode at different temperatures (298 K to 328 K).

The polarization plots obtained in HCl 1.0 M without and with the addition of 50 ppm of the tested compounds in the temperature range (298-328 K) are presented in Figure 7. The values of the corrosion current densities (I_{corr}), corrosion potentials of the steel (E_{corr}) and the inhibition efficiencies as a function of temperature are given in Table 7.

Table 7. Temperature effect on the electrochemical parameters of mild steel in HCl 1.0 M in the absence and the presence of 50 ppm of both compounds

Compounds	Temperature K	$-E_{corr}$ mV/Ag/AgCl	i_{corr} µA cm^{-2}	$-\beta_c$ mV dec^{-1}	β_a mV dec^{-1}	η_{PP} %
Blank	298	498	983	140	150	-
	308	491	1200	184	112	-
	318	475	1450	171	124	-
	328	465	2200	161	118	-
1BHP	298	489	207	131	124	78.9
	308	505	278	128	126	76.8
	318	519	372	121	123	74.3
	328	522	624	125	121	71.6
2BHP	298	472	132	121	128	86.6
	308	524	185	127	115	84.5
	318	516	269	126	117	81.4
	328	508	468	134	133	78.7

Based on the analysis of the results obtained, we find that:

- ✓ The corrosion current density values increase with temperature in the whole studied range. This is probably due to the acceleration of steel corrosion kinetics with increasing temperature.
- ✓ The curves in the cathodic part are parallel, explaining that H+ ions reduction on the steel surface is done according to the same pure activation mechanism.
- ✓ Inhibition efficiency η_{PP} (%) of the tested compounds decreases with the temperature increase. This can be explained by the positive contribution to the corrosion phenomenon.

This can be also explained by a slight change of equilibrium adsorption- desorption in favor of the desorption process thus decreasing the inhibitory power of the molecule [48,49].

3.2.4. Activation parameters of corrosion process

By studying the effect of temperature on the corrosion current density (i_{corr}) we can calculate the value of the activation energy (E_a) of the corrosion process, with different temperatures, in the absence and the presence of the inhibitors 1BHP and 2BHP, according to Arrhenius equation (12) [50].

$$\ln i_{corr} = \ln A - \frac{Ea}{RT} \qquad (12)$$

where i_{corr} is the corrosion current density, R is the noble gases constant and T is the absolute temperature. A is Arrhenius pre-exponential factor.

The variation of the logarithm of the corrosion current density as a function of the temperature reciprocal (1000/T) is given in Figure 8 in the absence and presence of 50 ppm of both glassy compounds. From Arrhenius relationship, we can calculate the activation energies which are given in Table 8. It is noteworthy that E_a values in the presence of both glassy compounds are higher than E_a value obtained for the free inhibitor solution. This increase in corrosion energy activation in the presence of inhibitors, associated with a decrease in the inhibition efficiency

At high temperatures, is frequently interpreted as due to the formation of an adsorption film of a physical nature, i.e. involving electrostatic interactions with the metal surface [51,52].

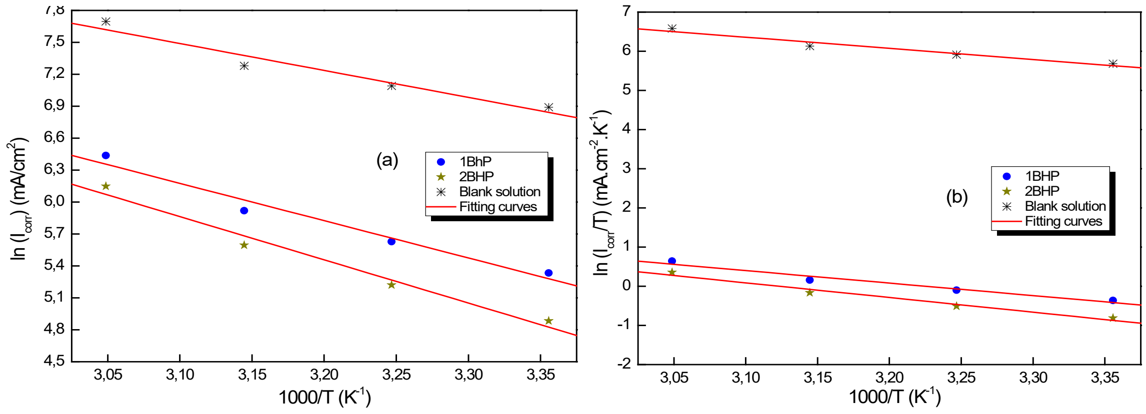

Fig. 8. Arrhenius diagrams for mild steel in HCl 1,0 M in the absence and the presence of 50 ppm of both glassy compounds/(a) of ln (i_{corr}) *vs.* 1000/T and (b) ln(i_{corr}/T) *vs.* 1000/T

Standard activation enthalpy values (ΔH_a) and activation entropy (ΔS_a) were calculated according to the following equation (13):

$$\ln\frac{icorr}{T} = (\ln (\frac{R}{Nh}) + \frac{\Delta Sa}{R}) - \frac{\Delta Ha}{RT} \tag{13}$$

where N is the Avogadro number and h is Planck's constant.

Figure 8 illustrates the variation of I_{corr}/T as a function of the temperature reciprocal for the blank solution and for a concentration of 50 ppm for both glassy compounds. The lines obtained have a slope equal to ($-\Delta H_a/R$) and an intercept equal to ($\ln(R/Nh)+\Delta S_a/R$). Owing to these lines, we can calculate ΔH_a andΔSa values. Enthalpies (ΔH_a) and entropies (ΔS_a) values are given in Table 8.

The positive signs of enthalpies (ΔH_a) reflect the endothermic nature of the process of steel dissolution. In fact, the increase of activation enthalpy corresponds to a decrease in the metal dissolution. The high and negative values of activation entropy, in the presence of the studied inhibitors, indicate a decline in the disorder during the formation of the metal complex/adsorbed species [53].

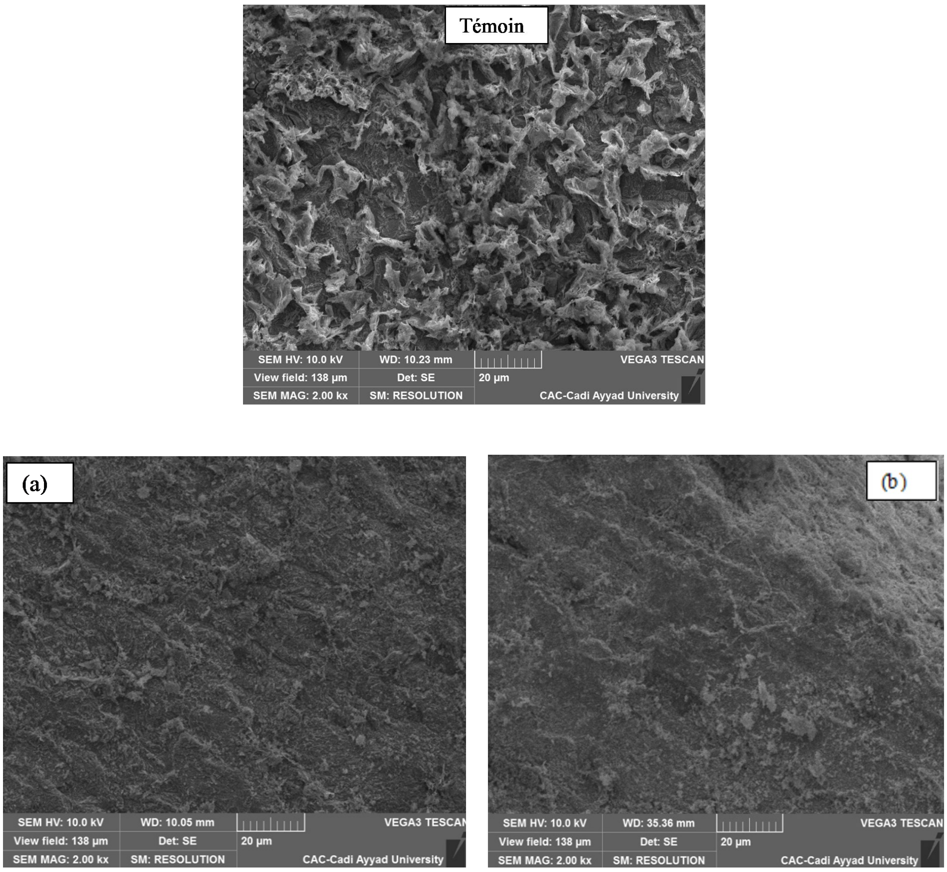

Fig. 9. MEB micrographs of mild steel surface after 6 hours of immersion in HCl 1.0 M at 298 K in the absence and the presence of both glassy compounds: 1BHP (a) and 2BHP (b)

Table 8. Values of the activation parameters E_a, ΔH_a and ΔS_a for mild steel in HCl 1.0 M without and with the addition of 50 ppm of both glassy compounds 1BHP and 2BHP

Medium		**E_a (KJ/mol)**	**ΔH_a (KJ/mol)**	**ΔS_a (KJ/mol.K)**
HCl 1.0 M	**Blank**	21.0	18.5	-126.0
	1 BHP	29.1	26.5	-111.9
	2 BHP	33.7	31.1	-100.0

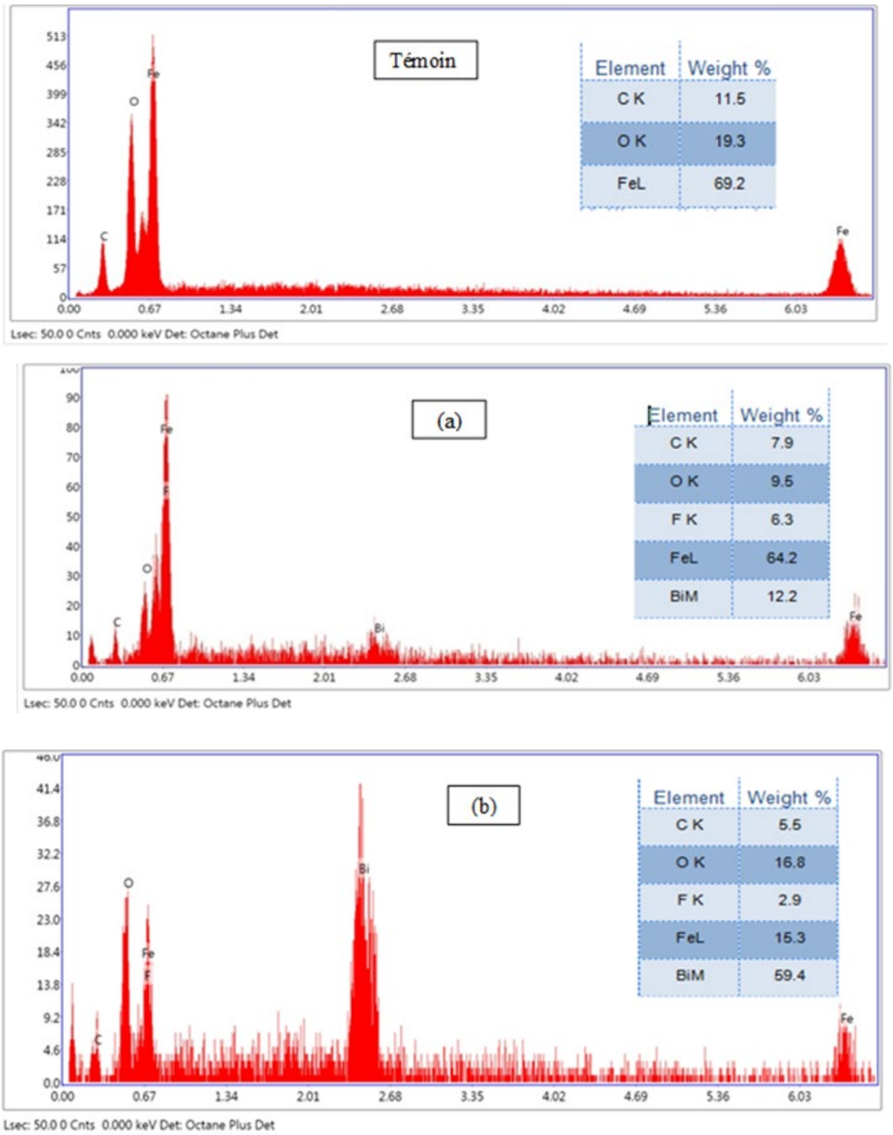

Element	Weight %
C K	11.5
O K	19.3
FeL	69.2

Element	Weight %
C K	7.9
O K	9.5
F K	6.3
FeL	64.2
BiM	12.2

Element	Weight %
C K	5.5
O K	16.8
F K	2.9
FeL	15.3
BiM	59.4

Fig. 10. Qualitative and quantitative analysis of mild steel by EDX, after 6 h of immersion in a blank solution of HCl 1.0 M and in the solution containing 50 ppm of 1BHP (a) and 2BHP (b)

3.2.5. Surface analysis

The corresponding MEB micrographs and EDX spectra of mild steel samples after 6 h of immersion in HCl 1.0 M at 298 K in the absence and the presence of both glassy compounds are presented in Figure 9.

The image of the surface of the mild steel after 6 h of immersion in HCl 1.0 M at 298 K shows clearly that the latter is under attack. The steel suffered from corrosion in the absence of the inhibitor. However, in the presence of both glassy compounds 1BHP and 2BHP, we note on the surface micrographs of steel after 6H of immersion in HCl 1.0 M solution at 298 in the presence of 50 ppm of both compounds 1BHP et 2BHP, that the surface is covered by a product in the form of a wafer, reflecting the adsorption of the glassy phase [54]. This observation shows that the inhibition is due to the formation of a stable and insoluble adhesive deposit that restricts electrolyte access to the surface of the steel. We realized EDX analyses in order to identify the different elements present on the mild steel surface. Figure 10 presents EDX spectrums. In the case of the blank, we note the formation of iron oxide and the apparition of an oxygen peak, emerging from the steel attack in HCl 1.0 M.

We note also, in the presence of 1BHP and 2BHP, a decrease in the carbon and oxygen peak and the presence of Bismuth and fluorine. These observations confirm that the glassy compounds decrease the steel corrosion by forming a layer, which restricts electrolyte access to the surface of the steel

4. CONCLUSION

Concluding the experimental part, it was clearly demonstrated that all techniques used, are able to characterize and to follow the corrosion inhibition process promoted by two glassy compounds: 1BHP and 2BHP was investigated. The corrosion rate of mild steel decreased with decreasing the inhibitor concentration to reach a minimum at 50 ppm. 1 BHP and 2BHP exhibited good inhibition properties for mild steel corrosion in 1.0 M HCl solution and their inhibition efficiency is inversely proportional to their concentration. The obtained results showed that 1 BHP and 2BHP acted as mixed-type inhibitors of mild steel corrosion in 1.0 M HCl. Electrochemical impedance spectroscopy (EIS) measurement results indicated that the resistance of the mild steel increased with inhibitor concentrations to reach a maximum at 50 ppm of 1BHP and 2BHP but 2BHP showed higher protection and performances than 1BHP. This may be due to the percentage increase in bismuth phosphate, which improves adsorption of 2HBP on a charged metal surface. The adsorption characteristics of 1BHP and 2BHP followed the isothermal adsorption model of Langmuir. The study of temperature effect on the inhibition efficiency shows that this one decreases with the temperature increase. Which confirms that the adsorption of both glassy compounds is made by an intermediate adsorption between physisorption and chemisorptions. Surface morphology studies confirmed the mitigation of mild steel corrosion by the formation of a protective film on the surface of the steel.

REFERENCES

[1] M. Ouakki, M. Galai, M. Cherkaoui, E. H. Rifi, and Z. Hatim, Anal. Bioanal. Electrochem. 10 (2018) 943.

[2] M. A. Amin, S. S. Abd El-Rehim, E. E. F. El-Sherbini, and R. S. Bayyomi, Electrochim. Acta 52 (2007) 3588.

[3] S. Bensaada, Corrosion (2003).

[4] A. Tazouti, M. Galai, R. Touir, M. Ebn Touhami, A. Zarrouk, Y. Ramli, M. Saraçoğlu, S. Kaya, F. Kandemirli, and C. Kaya, J. Mol. Liquid. 221 (2016) 815.

[5] G. Trabanelli, V. Caraaiti, in: N. G. Fatana, R. W. Dtaehle (Eds.), Advances in Corrosion Science and Technology, vol. 1, Plenum Press, New York, NY (1970) 147.

[6] A. Elbadaoui, M. Galai, M. Cherkaoui, and T. Guedira. Der Pharma Chem. 8 (2016) 214.

[7] L. Chafki, M. Galai, E. H. Rifi, R. Touir, M. Ebn Touhami, Z. Hatim, and A. Tazouti, J. Chem. Pharm. Res. 7 (2015) 44.

[8] M. Galai, M. El Gouri, O. Dagdag, Y. El Kacimi, A. Elharfi, and M. Ebn Touhami, J. Mater. Environ. Sci. 7 (2016) 1562.

[9] G. Saha, and N. Kurmaih, Corrosion 42 (1986) 233.

[10] M. Ouakki, M. Galai, M. Cherkaoui, E. H. Rifi, and Z. Hatim, J. Chem. Technol. Metallurgy (2020) 2.

[11] O. K. Aboia, and A. O. James, Corros. Sci. 52 (2010) 661.

[12] N. O. Eddy, and S. A. Odoemelam, Pigment and Resin Technol. 38 (2009) 111.

[13] M. Belfaquir, T. Guedira, S. M. D. Elyoubi, and J. L. Rehspringer, Science Lib Editions Mersenn. 5 (2013) N° 130303.

[14] H. Veisi, A. Khazaei, L. Heshmati, and S. Hemmati, Bull. Korean Chem. Soc. 33 (2012) 1231.

[15] A. Dhanapala, S. R. Boopathy, and V. Balasubramanian, J. Alloys. Compd. 523 (2012) 49.

[16] S. Hong, W. Chen, H. Q. Luo, and N. B. Li, Corros. Sci. 57 (2012) 270.

[17] M. Stern, and A. L. Geary, J. Electrochem. Soc. 104 (1957) 56.

[18] A. Bouckamp, User's Manual Equivalent Circuit, Ver. 4 (1993) 51.

[19] I. B. Obot, N. O. Obi-Egbedi, and N. W. Odozi, Corros. Sci. 52 (2010) 923.

[20] M. Ouakki, M. Rbaa, M. Galai, B. Lakhrissi, E. H. Rifi, and M. Cherkaoui, J. Bio- and Tribo-Corros. 4 (2018) 35.

[21] E. Ech-chihbi, M. E. Belghiti, R. Salim, H. Oudda, M. Taleb, N. Benchat, B. Hammouti, and F. El-Hajjaji, J. Surf. Interf. 9 (2017) 206.

[22] R. A. Prabhu, T. V. Venkatesha, B. M. Praveen, K. G. Chandrappa, and S. B. Abd Hamid, Trans. Indian Inst. Met. 67 (2014) 675.

[23] D. Frenkel, and B. Smit, Understanding Molecular Simulation: From Algorithms to Applications, 2nd Ed, Academic Press, San Diego (2002).

[24] M. Galai, M. Rbaa, Y. El Kacimi, M. Ouakki, N. Dkhirech, R. Touir, B. Lakhrissi, and M. Ebn Touhami, Anal. Bioanal. Electrochem. 9 (2016) 80.

[25] F. Mansfeld, M. W. Kending, and S. Tsai, Corrosion 37 (1981) 301.

[26] M. Rbaa, M. Galai, Y. El Kacimi, M. Ouakki, R. Touir, B. Lakhrissi, and M. Ebn Touhami, Portugaliae Electrochim. Acta 35 (2017) 323.

[27] H. Serrar, M. Galai, F. Benhiba, M. Ouakki, Z. Benzekri, S. Boukhris, A. Hassikou, A. Souizi, H. Oudda, and M. E. Touhami. J. Chem. Technol. Metallurg. 53 (2018) 324.

[28] K. Al Mamari, H. Elmsellem, K. Sebbar, A. Elyoussfi, H. Steli, M. Ellouz, Y. Ouzidan, A. Nadeem, E. M. Essassi, and F. El-Hajjaji, J. Mater. Environ. Sci. 7 (2016) 3286.

[29] M. Galai, H. Benqlilou, M. Ebn Touhami1, T. Belhaj, K. Berrami, and H. El Kafssaoui, Environ. Eng. Res. 23 (2018) 164.

[30] C. B. Verma, M. J. Reddy, and M. A. Quraishi, Anal. Bioanal. Electrochem. 6 (2014) 321.

[31] M. E. Belghiti, Y. Karzazi, A. Dafali, I. B. Obot, E. E. Ebenso, K. M. Emrane, I. Bahadur, B. Hammouti, and F. Bentiss, J. Mol. Liq. 216 (2016) 874.

[32] N. M'hanni, M. Galai, T. Anik, M. Ebn Touhami, E. H. Rifi, Z. Asfari, and R. Touir, Surface Coatings Technol. 310 (2017) 8.

[33] S. Jodeh, S. Al Masri, O. Hamed, M. Haddad, D. Jodeh, R. Salghi, S. Radi, J. Amarah, F. El-Hajjaji, and I. Warad, J. Mater. Environ. Sci. 7 (2016) 1037.

[34] X. Zheng, S. Zhang, W. Li, L. Yin, J. He, and J. Wua, Corros. Sci. 80 (2014) 383.

[35] A. K. Singh, and M. A. Quraishi, J. Appl. Chem. 40 (2010) 1293.

[36] M. Benabdellah, A. Aouniti, A. Dafali, B. Hammouti, M. Benkaddour, A. Yahyi, and A. Ettouhami, Appl. Surf. Sci. 252 (2006) 8341.

[37] N. C. Subramanyam, and S. M. Mayanna, Corros. Sci. 25 (1985) 163.

[38] N. Eldakar, and K. Nobe, Corrosion 36 (1981) 271.

[39] K. Kurosawa, and T. Fukushima, Corr. Sci. 29 (1989) 1103.

[40] Y. I. Kuznetsov, Prot. Met. 37 (2001) 101.

[41] S. D. Deng, X. H. Li, and H. Fu, Corros. Sci. 53 (2011) 760.

[42] M. Nooshabadi, and M. Ghandchi, J. Ind. Eng. Chem. 31 (2015) 231.

[43] K. Adardour, O. Kassou, R. Touir, M. Ebn Touhami, H. El Kafsaoui, H. Benzeid, M. Essassi, and M. Sfaira, J. Mater. Environ. Sci. 1 (2010) 129.

[44] M. Elayyachy, A. El Idrissi, and B. Hammouti, Corros. Sci. 48 (2006) 2470.

[45] E. Bayol, A. A. Gurten, M. Dursun, and K. Kayakırılmaz, Acta Phys. Chim. Sin. 24 (2008) 2236.

[46] A. Yurt, S. Ulutas, and H. Dal, Appl. Surf. Sci. 253 (2006) 919.
[47] M. Abdallah, Corr. Sci. 44 (2002) 717.
[48] I. B. Obot, and N. O. Obi-Egbedi, Corros. Sci. 52 (2010) 657.
[49] G. N. Mu, X. Li, and F. Li, Mater. Chem. Phys. 86 (2004) 59.
[50] U. F. Ekanem, S. A. Umoren, I. I. Udousoro, and A. P. Udoh, J. Matter. Sci. 45 (2010) 5558.
[51] M. Galai, M. El Gouri, O. Dagdag, Y. El Kacimi, A. Elharfi, and M. Ebn Touhami, J. Mater. Environ. Sci. 7 (2016) 1562.
[52] N. Gharda, M. Galai, L. Saqalli, M. Ouakki, N. Habbadi, R. Ghailane, A. Souizi, M. EbnTouhami, and Y. Peres-lucchese. Oriental J. Chem. 33 (2017) 1665.
[53] K. Dahmani, M. Galai, M. Cherkaoui, A. El hasnaoui, and A. El Hessni, J. Mater. Environ. Sci. 8 (2017) 1676.
[54] M. Yadav, S. Kumar, N. Tiwari, I. Bahadur, and E. E. Ebenso, J. Mol. Liq. 212 (2015) 151.